REPORT DOCUMENTATION PAGE

Form Approved
OMB No. 0704-0188

Public reporting burden for this collection of information is estimated to average 1 hour per response, including the time for reviewing instructions, searching existing data sources, gathering and maintaining the data needed, and completing and reviewing this collection of information. Send comments regarding this burden estimate or any other aspect of this collection of information, including suggestions for reducing this burden to Department of Defense, Washington Headquarters Services, Directorate for Information Operations and Reports (0704-0188), 1215 Jefferson Davis Highway, Suite 1204, Arlington, VA 22202-4302. Respondents should be aware that notwithstanding any other provision of law, no person shall be subject to any penalty for failing to comply with a collection of information if it does not display a currently valid OMB control number. **PLEASE DO NOT RETURN YOUR FORM TO THE ABOVE ADDRESS.**

1. REPORT DATE (DD-MM-YYYY)	2. REPORT TYPE	3. DATES COVERED (From - To)
29-12-2006	Final Technical Report	30-09-2004 to 31-03-2006

4. TITLE AND SUBTITLE

Efficient THz Sources Based on Cascaded Optical Down-conversion
In Orientation-patterned GaAs Structures

5a. CONTRACT NUMBER

5b. GRANT NUMBER
FA9550-04-1-0465

5c. PROGRAM ELEMENT NUMBER

6. AUTHOR(S)
M.M. Fejer, K. Vodopyanov, J. Schaar, P. Kuo

5d. PROJECT NUMBER

5e. TASK NUMBER

5f. WORK UNIT NUMBER

7. PERFORMING ORGANIZATION NAME(S) AND ADDRESS(ES)
Edward L. Ginzton Laboratory
Stanford University
Stanford, CA 94305-4088

8. PERFORMING ORGANIZATION REPORT NUMBER
SPO No. 30750

9. SPONSORING / MONITORING AGENCY NAME(S) AND ADDRESS(ES)
AFOSR
801 North Randolph Street, Room 732
Arlington, VA 22203-1977
Dr Gernot Pomrenke/NE

10. SPONSOR/MONITOR'S ACRONYM(S)

AFRL-SR-AR-TR-07-0076

12. DISTRIBUTION / AVAILABILITY STATEMENT
Approved for public release; distribution unlimited.

13. SUPPLEMENTARY NOTES
The view, opinions and/or findings contained herein are those of the author(s) and should not be construed as necessarily representing the official policies or endorsements, either expressed or implied, of the Air Force Office of Scientific Research or the U.S. Government.

14. ABSTRACT

The goal of this TIFT I-A program was to demonstrate an efficient room temperature source for THz imaging systems based on optical down-conversion in an orientation-patterned GaAs microstructure, incorporated into a resonant cavity, and pumped by a compact solid-state laser. Research was focused on (1) fabrication of quasi-phase-matched (QPM) GaAs microstructures with periodic reversal of crystalline orientation, including orientation-patterned GaAs (OP-GaAs), diffusion-bonded GaAs (DB-GaAs) and optically-contacted GaAs (OC-GaAs), (2) producing THz radiation in periodic GaAs structures outside the laser cavity using both optical rectification (using femtosecond optical pump pulses) and difference frequency generation (with picosecond pulses), and, finally (3) demonstration of efficient resonantly enhanced THz wave generation with GaAs inside the cavity of an optical parametric oscillator, where 1 mW of average THz power was produced at 2.8 THz.

15. SUBJECT TERMS
THz imaging system, orientation-patterned GaAs, micro-structured nonlinear optical materials, quasi-phasematched devices, frequency conversion, nonlinear optics

16. SECURITY CLASSIFICATION OF:			17. LIMITATION OF ABSTRACT	18. NUMBER OF PAGES	19a. NAME OF RESPONSIBLE PERSON Martin M. Fejer
a. REPORT	b. ABSTRACT	c. THIS PAGE		27	19b. TELEPHONE NUMBER (include area code) (650) 725-2160

Standard Form 298 (Rev. 8-98)
Prescribed by ANSI Std. Z39.18

1.   AFOSR CONTRACT OR GRANT NUMBER: FA9550-04-1-0465

2.   PERIOD COVERED BY REPORT: 09/30/2004 – 03/31/2006

3.   TITLE OF PROPOSAL: Efficient THz source based on cascaded optical down-conversion in orientation-patterned GaAs structures

4.   LIST OF MANUSCRIPTS SUBMITTED OR PUBLISHED UNDER AFOSR SPONSORSHIP DURING THIS REPORTING PERIOD:
   See attached Final Technical Report

5.   SCIENTIFIC PERSONNEL SUPPORTED BY THIS PROJECT AND DEGREES AWARDED DURING THIS REPORTING PERIOD:
   Faculty - M.M. Fejer
   Senior Staff - K. Vodopyanov, R. Route
   Post-Doctoral Scholars –
   Students –P. Kuo , J. Schaar

6.   REPORT OF INVENTIONS BY TITLE ONLY:
   None

7.   SCIENTIFIC PROGRESS AND ACCOMPLISHMENTS:
   See attached Interim Technical Report

8.   TECHNOLOGY TRANSFER:
   The goal of Phase I is the demonstration of critical technology for a compact, room temperature THz source based on a cascaded optical down-conversion process in orientation patterned (OP) GaAs structures. Technology transfer will occur during Phase II as we develop device structures consistent with AFOSR interests.

9.   CORRESPONDENCE ADDRESS:
   Martin M. Fejer, P.I.
   Ginzton Laboratory, Mail Code 4088   (tel) 650-725-2160
   Stanford University   (fax) 650-723-2666
   Stanford, CA 94305-4088   fejer@stanford.edu

Final Technical Report

on

Efficient THz source based on cascaded optical down-conversion in orientation-patterned GaAs structures

Authors:

M. M. Fejer, K. L. Vodopyanov, J. E. Schaar
Edward L. Ginzton Laboratory, Stanford University, Stanford, California 94305
J. S. Harris and X. Yu
Solid State and Photonics Laboratory, Stanford University, Stanford, California, 94305
D. Bliss and C. Lynch
Air Force Research Laboratory, Hanscom Air Force Base, Massachusetts, 01731
V. G. Kozlov
Microtech Instruments, Inc, Eugene, Oregon, 97401
Y.-S. Lee and W. C. Hurlbut
Department of Physics, Oregon State University, Corvallis, Oregon 97331

ABSTRACT

The goal of this TIFT project was to demonstrate an efficient room temperature source for THz imaging systems based on optical down-conversion in an orientation-patterned GaAs microstructure, incorporated into a resonant cavity, and pumped by a compact solid-state laser. Research was focused on (1) fabrication of quasi-phase-matched (QPM) GaAs microstructures with periodic reversal of crystalline orientation, including orientation-patterned GaAs (OP-GaAs), diffusion-bonded GaAs (DB-GaAs) and optically-contacted GaAs (OC-GaAs), (2) producing THz radiation in periodic GaAs structures outside the laser cavity using both optical rectification (using femtosecond optical pump pulses) and difference frequency generation (with picosecond pulses), and, finally (3) demonstration of efficient resonantly enhanced THz wave generation with GaAs inside the cavity of an optical parametric oscillator, where 1 mW of average THz power was produced at 2.8 THz.

SUBJECT TERMS

micro-structured nonlinear optical materials, quasi-phasematched THz coherent sources, orientation-patterned GaAs, frequency down-conversion, room temperature THz source.

Efficient THz source based on cascaded optical down-conversion in orientation-patterned GaA structures
TIFT-AFOSR FINAL TECHNICAL REPORT
December 2006

PROGRAM OBJECTIVE: The goal of this TIFT project was to demonstrate an efficient room temperature source for THz imaging systems based on optical down-conversion in an orientation-patterned GaAs microstructure, incorporated into a resonant cavity, and pumped by a compact solid-state laser. Research was focused on (1) fabrication of GaAs microstructures with periodic reversal of crystalline orientation, including orientation-patterned GaAs (OP-GaAs), diffusion-bonded GaAs (DB-GaAs) and optically-contacted GaAs (OC-GaAs), (2) producing THz radiation in periodic GaAs structures outside the laser cavity using both optical rectification (femtosecond optical pulses) and difference frequency generation (picosecond pulses), and finally, (3) demonstration of efficient resonantly enhanced THz wave generation with GaAs inside the cavity of an optical parametric oscillator, where 1 mW of average THz power was produced at 2.8 THz.

RESEARCH TEAM MEMBERS:

*   **Stanford University:** Prof. Martin M. Fejer (P.I.), Prof. James S. Harris, Dr. Konstantin Vodopyanov, Joseph Schaar
*   **Air Force Research Laboratory, Hanscom Air Force Base, Massachusetts:** Dr. D. Bliss, Dr. C. Lynch
*   **Oregon State University:** Prof. Y-S. Lee, Dr. W.C. Hurlbut
*   **Microtech Instruments, Inc.:** Dr. V.G. Kozlov

FINANCIAL EXECUTION: The award amount for this program was $ 1,210,577, all of which was expended and off the government books by the end of the program on 31 March 2006.

SCIENTIFIC APPROACH: To achieve the program scientific objectives, the TIFT participants and collaborators worked along the following lines: In the field of GaAs material fabrication, Stanford and collaborators at Hanscom AFB focused on fabrication of orientation-patterned GaAs (OP-GaAs) structures. Stanford was using MBE and photolithography to create orientation templates, and Hanscom AFB was growing thick films on these templates by hydride-vapor-phase epitaxy. Additionally, researchers at Microtech Instruments worked on developing alternative technology for QMP GaAs for THz applications, namely optically-contacted GaAs (OC-GaAs). We also used in our THz experiments, diffusion-bonded GaAs samples developed and fabricated at Stanford as a result of previous scientific programs targeting mid-IR applications. At Oregon State University, we performed first trials on THz generation in GaAs using femtosecond optical pulses in the 2-4 μm range from an optical parametric amplifier. In this experiments, we tested the quality of GaAs samples and compared the performance of GaAs-based THz devices with theory (tuning curves and optical-to-THz conversion efficiency). Also, detrimental high-order nonlinear effects were measured in GaAs, using high-intensity fs pulses. Finally, at Stanford, we performed THz-wave generation using a near-degenerate optical parametric oscillator (OPO) operating near 2.1 μm, as a pump source. Three types of experiment were carried out: (i) GaAs

outside the cavity of the OPO, (ii) GaAs inside the OPO cavity and only one of the two OPO waves resonates, and finally, (iii) with GaAs inside the OPO cavity and with both of the two OPO waves resonating.

CONCLUSIONS AND RECOMMENDATIONS FOR FURTHER STUDIES:

Overall, this 18-months DARPA-AFOSR program has been highly successful in developing new methods for efficient generation of THz radiation. We successfully developed fabrication of quasi-phase-matched GaAs microstructures with periodic reversal of crystalline orientation, suitable for THz generation, including orientation-patterned GaAs and optically-contacted GaAs. We have generated terahertz radiation by both optical rectification of femtosecond laser pulses and by difference–frequency mixing of the signal and idler waves of a picosecond optical parametric oscillator. By varying the QPM period of GaAs, we were able to generate nearly monochromatic THz radiation between 0.5 and 3.5 THz, with a bandwidth of 100-300 GHz. The THz beam was nearly diffraction limited, and the spatial quality of the beam was measured with a room-temperature pyro-electric camera. We also measured 1st, 3rd, and 5th-order quasi-phasematching peaks using a single OC-GaAs sample, which makes this sample useful for generating multiple THz frequencies. We observed two additional optical satellites spaced by THz frequency, which is the evidence of the cascading effect: with each cascade the energy is additionally transferred to the THz wave. With an optimized OPO cavity we expect to generate 8 cascades. Resonant enhancement of optical waves inside the OPO cavity will further significantly increase the optical-to-THz conversion efficiency. In the doubly resonant OPO configuration, both the signal and idler waves were resonantly enhanced. We increased the optical-to-THz conversion efficiency by 20× over the SRO performance with an average output power of 1 mW at 2.8 THz. We developed a novel type-II linear doubly resonant OPO which avoided back-conversion, and we are currently lowering the OPO losses to improve the average THz output power. Approval of funding for TIFT phase II will enable scaling of THZ average power to 10–100 mW in our system.

HIGHLIGHTS:

1) QPM GaAs material fabrication for THz generation

Significant improvements in OP-GaAs template quality and hydride vapor phase epitaxy (HVPE) thick film growth were made. High quality, low surface roughness templates were grown reproducibly, while the subsequent HVPE growth for bulk samples achieved thicknesses up to 750 μm in one step and up to 1.2 mm in 3 steps.

Loss characterizations of thick-film OP-GaAs showed improved uniformity across the sample and losses in recent samples as low as 0.005-0.01 cm^{-1} at 2 μm

Technology of optically-contacted GaAs (OC-GaAs) was developed. The main advantage of the OC-GaAs (as compared to OP-GaAs) for THz generation is that there are no aperture limitations. Stacks of OC-GaAs as thick as 6 mm (along the beam k-vector) were achieved with one-inch aperture.

2) Broadly tunable quasi-monochromatic THz output

THz wave generation was demonstrated for the first time in QPM GaAs

By varying the QPM period of GaAs, we were able to generate (by both – optical rectification and difference frequency mixing) nearly monochromatic THz radiation between 0.5 and 3.5 THz, with a bandwidth of 100-300 GHz

We measured 1st, 3rd, and 5th-order quasi-phasematching peaks using a single OC-GaAs sample, which makes this sample useful for generating multiple THz frequencies.

The THz beam was nearly diffraction limited, and the spatial quality of the beam – close to Gaussian.

Detrimental high-order nonlinear effects (2-photon, 3-photon absorption, nonlinear refraction) were measured in GaAs, using high-intensity fs pulses.

3) Terahertz generation inside the OPO cavity

Intracavity THz wave generation was demonstrated for the first time in GaAs. QPM GaAs was placed inside the resonator of a near-degenerate PPLN OPO.

In the doubly resonant OPO configuration the optical-to-THz conversion efficiency was increased by 20× over singly resonant performance, with an average output power of 1 mW at 2.8 THz.

4) Observation of THz cascading effect in the optical-to-THz frequency conversion

We observed two additional optical satellites spaced by THz frequency, which is the evidence of the cascading effect: with each cascade the energy is additionally transferred to the THz wave. With an optimized OPO cavity we expect to generate 8 cascades and beat Manley-Rowe limit by about the same factor.

TRAINING OF GRADUATE STUDENTS:

At the end of this 18-months-year TIFT program, 1 graduate student has completed a Ph.D. dissertation and an additional 2 have been supported.

PERSONNEL SUPPORTED:

Stanford
- Faculty: 2
- Staff: 1
- Students: 2
- Post-Docs: 0

Hanscom AFB
- Staff: 2
- Students: 0
- Post-Docs: 0

Oregon State University
- Faculty: 1
- Staff: 0
- Students: 1 supported (1 Ph. D. awarded)
- Post-Docs: 0

Microtech, Inc.
- Staff: 2

PAPERS PUBLISHED: 20

Journal Papers

1. G. Imeshev, M. E. Fermann, K. L. Vodopyanov, M. M. Fejer, X. Yu, J. S. Harris, D. Bliss, and C. Lynch, "High-power source of THz radiation based on orientation-patterned GaAs pumped by a fiber laser", Opt. Express 14, 4439-4444 (2006)

2. K. L.Vodopyanov, M. M. Fejer, X. Yu, J. S. Harris, Y.-S. Lee, W. C. Hurlbut, V. G. Kozlov, D. Bliss, and C. Lynch, "Terahertz wave generation in quasi-phase-matched GaAs, Appl. Phys. Lett.", 89, 141119 (2006)

3. Yun-Shik Lee, W. C. Hurlbut, K. L. Vodopyanov, M. M. Fejer, and V. G. Kozlov, Generation of multicycle terahertz pulses via optical rectification in periodically inverted GaAs structures, Appl. Phys. Lett. 89, 181104 (2006)

4. K. L. Vodopyanov, "Optical generation of narrow-band terahertz packets in periodically inverted electro-optic crystals: conversion efficiency and optimal laser pulse format," Opt. Express 14, 2263-2276 (2006)

5. W. C. Hurlbut, Yun-Shik Lee, K. L. Vodopyanov, P. S. Kuo, and M. M. Fejer, Multi-photon absorption and nonlinear refraction of GaAs in the mid-infrared, Optics Letters - in press

Conferences

1. K. L. Vodopyanov, D. Simanovskii, M. M. Fejer, "Terahertz-wave generation in periodic GaAs structures" , Advanced Solid State Photonics (ASSP), Vienna, Jan 2005

2. K. L. Vodopyanov, D. Simanovskii, M. M. Fejer, V.G. Kozlov, Y.-S. Lee "Tunable narrow-band terahertz-wave generation in periodic GaAs via synchronous optical rectification", Optical Terahertz Science and Technology (OTST), Orlando, FL, Mar 2005

3. K. L. Vodopyanov, D. M. Simanovskii, M. M. Fejer, V.G. Kozlov, Y.-S. Lee, "Terahertz-wave generation in periodically-inverted GaAs," CLEO/QELS, Baltimore MD, May 2005

4. K. L. Vodopyanov "Periodic gallium arsenide and its applications for tunable mid-IR and THz wave generation", invited talk, Nonlinear Wave Physics Conf., St. Petersburg- N. Novgorod, Russia, Aug 2005

5. K. L. Vodopyanov "A new terahertz-wave source based on periodically-inverted gallium arsenide", invited talk. NATO workshop on Middle Infrared Coherent Sources, Barcelona, Spain, Nov 2006

6. V.G. Kozlov, D. Bliss, K.L. Vodopyanov, M.M. Fejer, W. Hurlbut, Y.-S. Lee, "Frequency tunable THz source based on optical down conversion in orientation patterned GaAs", Joint 30th International Conference on Infrared and Millimeter Waves, Williamsburg, VA, USA, Sept. 2005, p.632-3 vol. 2

7. Yun-Shik Lee, K. L. Vodopyanov, W. C. Hurlbut, J. R. Danielson, V. G. Kozlov, D. F. Bliss, and M. M. Fejer, "Generation of multi-cycle THz- pulses via optical rectification in periodically inverted GaAs," Photonics West, San Jose, CA, Jan. 2006

8. G. Imeshev, M. E. Fermann, K. L. Vodopyanov and M. M. Fejer, X. Yu and J. S. Harris, D. Bliss, and D. Weyburne, "High-power source of THz radiation based on orientation-patterned GaAs pumped by a fiber laser", Advanced Solid State Photonics (ASSP), Lake Tahoe, Jan 2006

9. W. C. Hurlbut, K. L. Vodopyanov, M. M. Fejer, V.G. Kozlov, and Yun-Shik Lee, "Quasi-phasematched THz generation in GaAs," CLEO/QELS, Long Beach, CA, June 2006

10. W. C. Hurlbut, K. L. Vodopyanov, P. S. Kuo, M. M. Fejer, and Yun-Shik Lee, "Multi-photon absorption and nonlinear refraction of GaAs in the mid-infrared," CLEO/QELS, Long Beach, CA, June 2006

11. Konstantin Vodopyanov, Paulina Kuo, Joe Schaar, Xiaojun Yu, Martin Fejer, Vladimir Kozlov, Yun-Shik Lee, David Bliss, Candace Lynch, Gennady Imeshev, and Martin Fermann, "Mid-IR and THz wave generation using quasi-phase-matched GaAs structures", invited talk, Laser Optics 2006 Conf., S-Petersburg, Russia, June 2006

12. Konstantin L. Vodopyanov, Joe Schaar, Xiaojun Yu, Martin Fejer, Jim Harris, Vladimir Kozlov, Yun-Shik Lee, Gennady Imeshev, Martin Fermann, David Bliss, and Candace Lynch, "Tunable THz source based on quasi-phase-matched GaAs", Europhoton 2006 Conf., Pisa, Italy, Sept. 2006

13. Konstantin L. Vodopyanov, J. Schaar, M.M. Fejer, X.Yu, J. Harris, Y.-S. Lee, V.G. Kozlov, G. Imeshev, M.Fermann, D. Bliss, and C. Lynch, "Tunable THz source based on frequency conversion in quasi-phase-matched GaAs", invited talk, Optics East, Boston, MA, Oct. 2006

14. Konstantin Vodopyanov, Joe Schaar, Martin Fejer, Xiaojun Yu, J.S. Harris, Vladimir Kozlov, Yun-Shik Lee, Gennady Imeshev, Martin Fermann, David Bliss, and Candace Lynch, "Terahertz wave generation in orientation-patterned GaAs", invited talk, Laser Physics Conference, Ashtarak, Armenia, Oct. 2006

Book Chapters

K. L. Vodopyanov, "Tunable THz Sources Based On Quasi-Phase-Matched Gallium Arsenide", in Middle Infrared Coherent Sources, NATO Science Series: eds: M. Ebrahimzadeh and I.T. Sorokina, Springer, 2007 (in print)

MAJOR ACCOMPLISHMENTS:

1. QPM GaAs material fabrication for THz generation

THz waves (1THz = 10^{12} Hz) can be used for numerous applications including real–time imaging (THz waves have, in many occasions, much smaller scattering than the optical waves and thus can penetrate many materials) and spectroscopy, both in condensed and gaseous phase, because of the richness of the absorption spectra in the THz frequency range. Parametric frequency down–conversion of optical pulses is a well–known, but currently inefficient, method of generating THz radiation. By this technique, one can generate either quasi–monochromatic THz radiation using using difference frequency generation (DFG) or broadband THz transients using optical rectification (OR). THz wave generation in GaAs was first demonstrated in in 1972, where the authors used difference frequency generation between the two CO_2 laser lines.[1]

GaAs has many attractive properties for THz generation such as a small THz absorption coefficient, large coherence length, large thermal conductivity, large nonlinear coefficient, and well–established manufacturing techniques (developed for mid-IR applications at Stanford and Hanscom AFB) to achieve quasi phase-matching (QPM). The absorption in GaAs ranges from 0.5–4.5 cm^{-1} for 1–3 THz and is more than an order of magnitude smaller than that in lithium niobate. The coherence length between the optical and THz waves in GaAs is large due to (i) large THz wavelength and (ii) small mismatch between the optical–group and THz–phase refractive indices. As a numerical example, the room temperature group index at λ=2.1 µm is 3.42 and the phase index at 1-2 THz is 3.6. This corresponds to an index mismatch of Δn = 0.18 which results in a required QPM period in GaAs of 1-1.5 mm, to achieve efficient interaction between optical and THz waves.
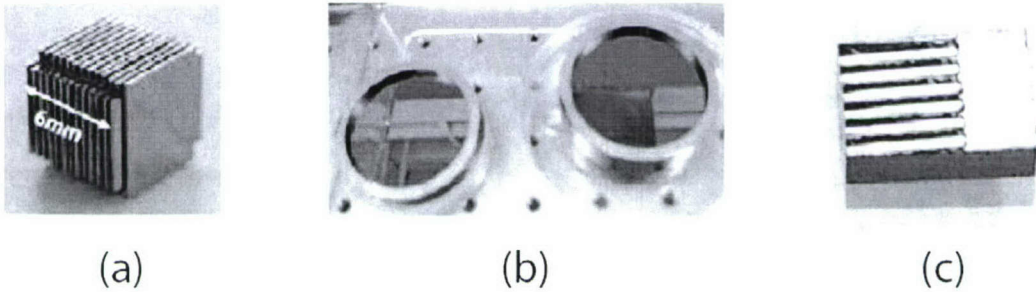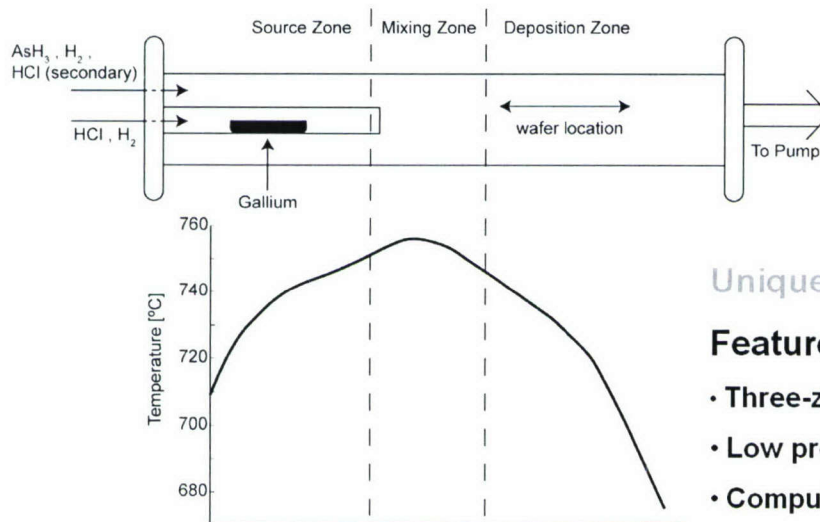

(a)   (b)   (c)

Fig. 1. Three different QPM GaAs samples: (a) DB–GaAs, sample A, with dimensions 10 mm×10 mm×6 mm and QPM period Λ= 504 µm. (b) OC–GaAs, samples B and C, with diameters of 5.08 cm and Λ=2 mm. (c) OP–GaAs, sample L5, with thickness of 800 µm, width of 6 mm, length of 5 mm, and Λ= 704 µm.

We used three different types (Fig. 1) of microstructured QPM GaAs: orientation–patterned GaAs (OP–GaAs), diffusion–bonded GaAs (DB–GaAs), and optically–contacted GaAs (OC–GaAs). The former structure is the most attractive because it is all-epitaxially-grown and allows the most precise definition of periodic structure, however it suffers from limited aperture (height).

OP–GaAs samples

A key part of the project on the material side was the growth of thick-film OP-GaAs samples with various QPM periods suitable for THz applications. In the OP-GaAs fabrication process, a photolithographically defined template of inverted GaAs (on top of the non-inverted GaAs substrate) is created, using first molecular beam epitaxy (MBE) and the photolithography, to a few microns in thickness. Secondly, hydride vapor phase epitaxy (HVPE), Fig. 2, grows the QPM structure to a thickness which is suitable for THz applications.

Unique System @ AFRL

Features:

· **Three-zone furnace and control**

· **Low pressure operation**

· **Computer control of mass flow**

· **Gas handling system for corrosive gases**

· **Alarm system for AsH$_3$**

· **Facility ambient is at negative pressure**

Overall Reaction:

$$GaCl + AsH_3 = GaAs + HCl + H_2$$

At 3.8 torr – uncracked arsine is favored → growth is faster
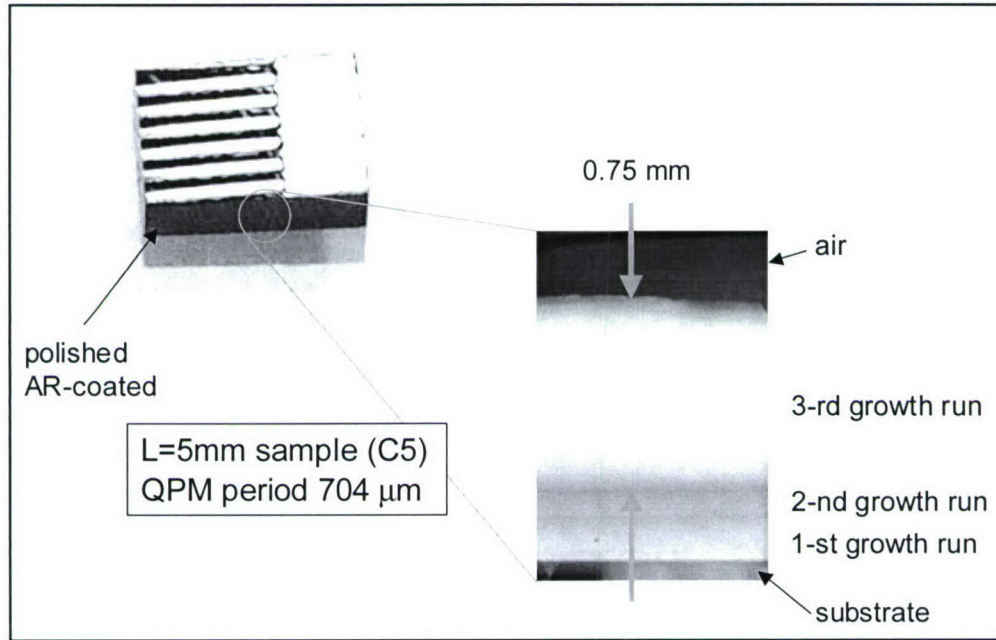
Fig. 2. Hydride Vapor Phase Epitaxy process at Hanscom AFB

Fig. 3. OP-GaAs sample for the optical THz generation. The inset shows optical transmission obtained with a near-infrared (λ~ 1μm) microscope. There were 3 runs of HVPE thick-film growth, the last one being the most successful, providing the useful thickness of 0.75 mm.

The thick films (up to ~1-mm) were grown (by the group of Dr. David Bliss of Hanscom Air Force Base) by HVPE on templates grown at Stanford by a combination of MBE and photolithography. Steady improvement in the growth of thick film OP-GaAs has occurred over the course of the program. Thicknesses over 1mm have been achieved in multi-step HVPE growths. Recently, OP-GaAs thick films with thicknesses up to 750-μm have been grown in a single step. The single-step growth runs avoid growth interruptions, which have been associated with excess loss at the boundary between two growths. In three steps, > 1.2 mm thickness was achieved (Fig. 3).

Recent thick films have also shown successful propagation of periods as small as 40mm through 700-μm-thick films. Smaller periods have a tendency to "close-over" (terminate prematurely) due to the close proximity of domain walls. A slight imbalance between the growth rates of the two phases causes one of the orientations to overgrow the other, resulting in termination of the quasi-phasematching grating. It was determined that the GaAs phase originating from the substrate of the template was more likely to overgrow the other phase and "dominate" the growth. By choosing the pattern of the template to have more areas of the less dominant phase, less overgrowth was observed and smaller periods grew to larger thicknesses before closing over.

DB–GaAs samples

DB–GaAs samples are made of N individual GaAs plates and by periodically rotating every other plate by 90° creates a sample with (N/2) QPM periods. GaAs plates are brought together under pressure while high temperatures are applied which allows diffusion to occur across the interface creating a nearly–monolithic structure. The DB–GaAs sample we used (sample A) for THz generation had an aperture of 10 mm× 10 mm, length of 6.05 mm, QPM period of 504 μm, and was constructed of 24 GaAs plates (Fig. 1a). Diffusion-bonded GaAs samples were developed and fabricated at Stanford as a result of previous scientific programs targeting mainly mid-IR applications.

OC–GaAs samples

Another type of microstructured QPM GaAs was OC–GaAs which was similar to DB–GaAs since the construction involves separate plates of GaAs which are brought together with a 90° domain rotation between neighboring plates. However, the plates were not heated to create a uniform crystalline structure. The individual GaAs wafers were 5.08 cm (2") in diameter and 1 mm thick.

In a device constructed by Microtech Instruments, Inc., one plate was dragged onto another (Fig. 4) in a low–pressure environment creating interfaces which were optically uniform and held together by Van der Waals interactions. OC–GaAs samples had more aperture than the DB–GaAs sample, better optical transparency for the IR waves, but the QPM period was fixed at 2 mm by the 1–mm–thick GaAs plates.
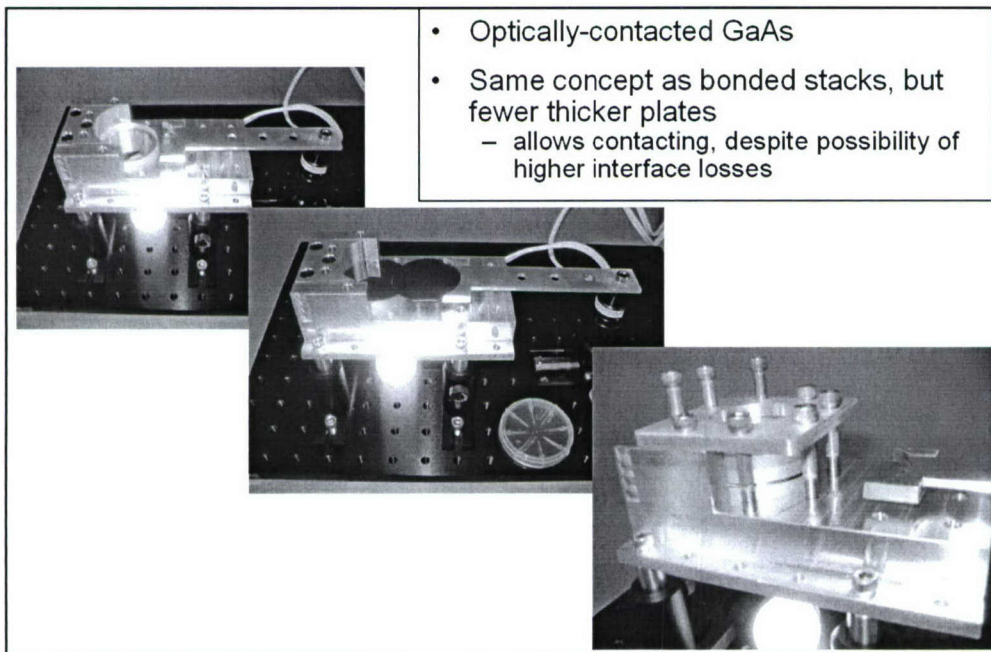

Fig. 4. Fabrication process of the optically-contacted GaAs

Comparison of three types of QPM GaAs shows that very low absorption (0.01 cm^{-1}) can be achieved in both OP-GaAs and OC-GaAs at λ=2 μm wavelength. Absorption in the DB-GaAs was found to be larger: ~ 0.1 cm^{-1}, because the technology was not very well developed at the time it was produced. Once again, while OC-GaAs and DB-GaAs provide larger apertures (and hence smaller clipping losses), OP-GaAs gives practically unlimited length of the samples and has more reproducible technology and allows lithographic definition of QPM gratings. For example, nonuniform (chirped) or fanned-out gratings can be easily produced via OP-GaAs technology. Main parameters of our QPM GaAs samples are listed in Table 1.

Table 1. QPM GaAs Samples Used for THz Generation

Sample Name	QPM Type	QPM Period (μm)	Length (mm)	Aperture (mm × mm)
A	DB–GaAs	504	6	8×8
B	OC–GaAs	2000	2	20×20
C	OC–GaAs	2000	4	20×20
D3	OP–GaAs	1277	3	6×0.4
D10	OP–GaAs	1277	10	6×0.4
E3	OP–GaAs	759	3	6×0.4
E6	OP–GaAs	759	6	6×0.4
E10	OP–GaAs	759	10	6×0.4
F5	OP–GaAs	564	5	6×0.4
G5	OP–GaAs	2326	5	6×0.4
G10	OP–GaAs	2326	10	6×0.4
H3	OP–GaAs	932	3	6×0.4
H5	OP–GaAs	932	5	6×0.4
H10	OP–GaAs	932	10	6×0.4
I3	OP–GaAs	704	3	6×0.4
I5	OP–GaAs	704	5	6×0.4
I10	OP–GaAs	704	10	6×0.4
J3	OP–GaAs	932	3	6×0.8
J5	OP–GaAs	932	5	6×0.8
J10	OP–GaAs	932	10	6×0.8
K3	OP–GaAs	1717	3	6×0.8
K5	OP–GaAs	1717	5	6×0.8
K10	OP–GaAs	1717	10	6×0.8
L3	OP–GaAs	704	3	6×0.8
L5	OP–GaAs	704	5	6×0.8
L10	OP–GaAs	704	10	6×0.8
M3	OP–GaAs	564	3	6×0.8
M5	OP–GaAs	564	5	6×0.8

2. THz generation via optical rectification using femtosecond IR pulses

THz generation using fs OPA system

In our first set of experiments we produced THz waves in GaAs via optical rectification (Fig. 5). Optical pulses from a OPA/DFG system, tunable in the range 2-4.4 μm, were generated using tunable parametric amplifier (OPerA, Coherent Inc.) pumped by 800-nm Ti:Sapphire pulses after a regenerative amplifier (Legend, Coherent Inc.). To achieve λ> 3 μm wavelengths, an additional difference frequency generation (DFG) stage was used. Typical pulse durations were ~100 fs, repetition rate 1 kHz, and pulse energy up to 3 μJ. The >2 μm pump wavelength range was chosen to avoid two-photon absorption (2PA) in GaAs (2PA edge is at ~ 1.75 μm), which creates additional losses both at pump wavelength and at terahertz frequencies (in the latter case because of induced absorption due to generated free carriers).

We have used [2] two types of QPM GaAs samples: (i) diffusion-bonded GaAs (DB-GaAs), and (ii) orientation-patterned GaAs (OP-GaAs).

Fig.5. Illustration of THz generation by optical rectification of femtosecond pulses in an EO crystal with periodically inverted sign of χ(2).

The optical pump beam with a beam size (1/e2 intensity radius) ranging between w=300 μm and 1.5 mm, propagated along the [110] direction of GaAs. A Picarin lens was used to collect the THz radiation to the liquid He-cooled silicon bolometer which measured the average power of THz pulses. A black polyethylene filter was used to block optical radiation. To measure the spectral properties of THz radiation, we have used a Michelson interferometer (Fig. 6). We utilized a 25-mm-thick mylar film as a beam splitter and two gold mirrors as end reflectors. One of the mirrors was mounted on a computer-controlled motorized stage. By computing the amplitude of the Fourier transform of the interferograms we extracted the power spectra of the generated THz radiation.

Fig. 7 shows both original interferograms and computed spectra for different samples and different pump wavelengths. The spectra were noticeably distorted by water vapor absorption (also shown in Fig.7). Interestingly, for sample D10 with the largest QPM period, 1277 μm, we observed (Fig. 7d) a second peak at ~2.6 THz which is likely to be the 3-rd order QPM peak, at approximately three times the frequency of the main peak. The amplitudes of both peaks are comparable. Efficiency reduction ($1/3^2$)

due to the 3rd order QPM is offset by the ν_{THz}^2 factor which appears in the expression for the efficiency of any DFG-like process.
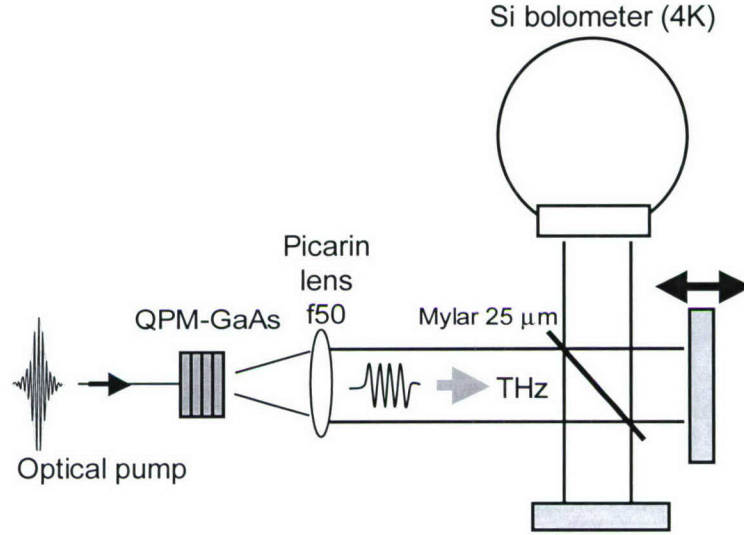

Fig..6. Experimental setup for THz generation and Michelson interferometry.
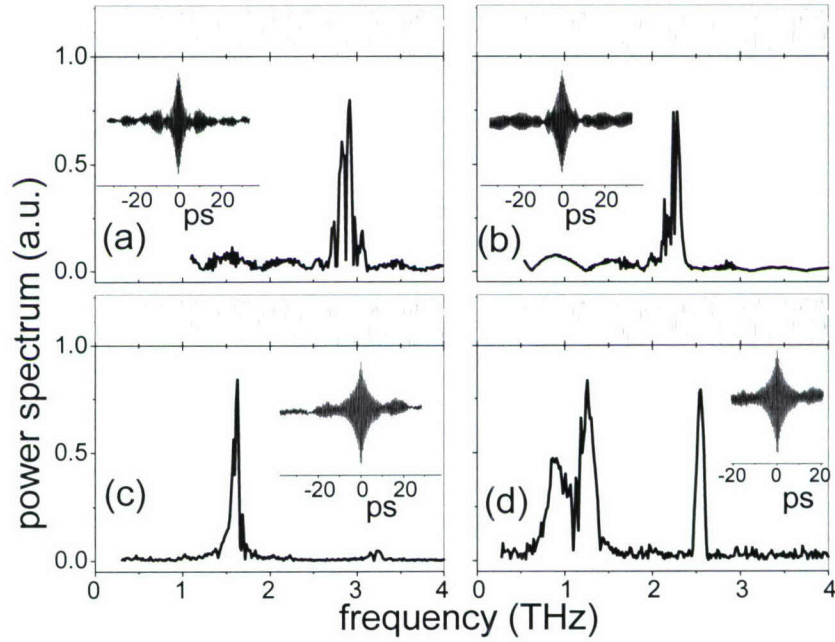

Fig. 7. Spectra of THz pulses obtained by Michelson interferometry. (a) Sample A, pump at 2.03 μm (b) sample A, pump at 3.5 μm (c) sample E10, pump at 4.4 μm; (d) sample D10, pump at 4.4 μm. The spectra are distorted by water vapor absorption (HITRAN water transmission spectrum for 10 cm path is shown on top of each plot). Insets show original interferograms.

The central frequency of terahertz radiation, produced by the QPM optical rectification is given by $\nu THz = c/\Lambda\Delta n$ and corresponds to the zero wave-vector mismatch condition. The spectral width of terahertz wavepackets is determined by[3] $\Delta\nu THz = c/L\Delta n$. Experimentally, we observed central frequencies and bandwidths of THz pulses that are in good agreement with these predictions based on known GaAs dispersion relations; for GaAs, $n$group varies[4] between 3.43 ($\lambda = 2\mu m$) and 3.33 (4.4 μm). By changing the pump wavelength or GaAs QPM period, we generated THz wave packets with central frequencies between 0.9 and 3 THz. The tuning curves for two different optical pump wavelengths are shown in Fig. 8 and match the theory pretty well.

Fig. 8 THz central frequency as a function of the OP-GaAs QPM period. (a) Pump wavelength at 4.4 µm and (b) at 2.13 µm .

We found that the THz beam propagated collinearly with respect to the optical pump and was close to diffraction-limited (a pinhole method was used to measure the far-field THz beam size). Fig. 9. shows optical-to-terahertz conversion efficiency, ηTHz, as a function of peak pump intensity, $I0$, inside the sample, at $\lambda = 3.5\text{-}4.4$ µm pump wavelength. The pump beam size varied in this case between 810 µm (open circles), 520 µm (closed circles), and 300 µm (crossed circles). One can see that the linear dependence (sample A) of ηTHz, expected by theory, rolls off for $I0 > 2$ GW/cm2. This roll-off behavior was also observed at similar intensities at shorter, $\lambda\sim 2$ µm pump. The onset of saturation is most likely due to nonlinear refraction ($n2$) in GaAs which induces self-phase modulation and self-focusing of the optical pulses. Indeed, we have measured $n2I\approx 1.5\cdot 10\text{-}4$ cm2/GW for GaAs at 3.5 µm and estimated that at $I0 = 2$GW/cm2 and L(GaAs)=6 mm, the nonlinear phase shift at beam center reaches $\sim\pi$.

Terahertz conversion efficiencies for the OP-GaAs samples D3 and E5 are very similar to each other and are smaller, by a factor of ~ 3.5, than that of the A sample (in both cases the pump was at 3.5 µm, central frequencies at 1.5 and 1.76 THz, correspondingly). We attribute smaller THz outputs in D3 and E5 to the beam clipping: their limiting dimension (height) is only 0.4 mm, comparable to THz wavelengths ($\sim 200\mu m$). Also, for the sample A, pump polarization was aligned along [111], while for D3 and E5 it was along [110]; in the former case, the nonlinear optical coefficient was larger: $\sqrt{4/3}d_{14}$ vs. d_{14}.

In the A sample, we generated 0.66 nJ of output at 2.2 THz, with 2.3 µJ of pump pulse energy ($w = 300\mu m$), which corresponds to optical-to-terahertz conversion efficiency of 2.9×10^{-4}, internal efficiency 8.7×10^{-4} (the samples were un-coated) and photon conversion efficiency of 1.1% (internal photon efficiency 3.3%). These efficiencies are in accord with the calculated values, based on the known nonlinear optical coefficient for optical rectification $d_{eff} = 2/\pi\times d_{14} = 2/\pi\times 46$ pm/V . We note that the measured conversion efficiency can be affected by water vapor absorption along the beam path (~ 30cm).

11
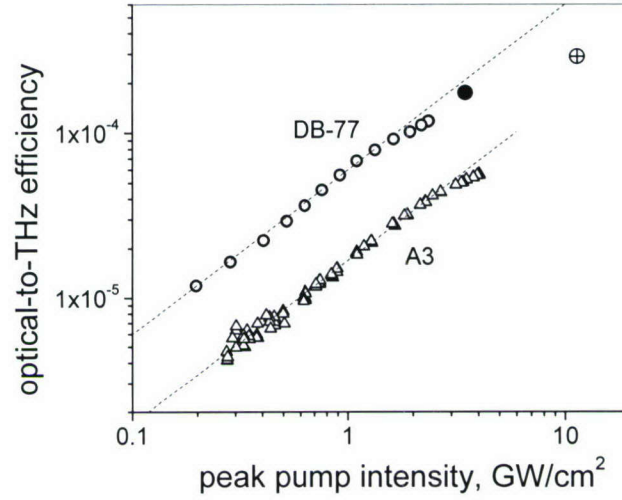
Fig. 9. Optical-to-terahertz conversion efficiency as a function of peak pump intensity for the sample A (central frequency ~2.2 THz, circles) and D3 (central frequency ~1.5 THz, triangles). The average pump beam size was 810 μm (open circles), 520 μm (closed circles), 590 μm (triangles), and 300 μm (crossed circles). The pump wavelength was 3.5 μm (open circles and triangles) and 4.4 μm (filled and crossed circles). Dashed lines – linear fits.

THz generation using fs fiber laser

In our second set of THz experiments[5], we used as a pump, a recently developed compact all-fiber source that generates femtosecond pulses at the wavelength near 2 μm. Fiber-based sources of short optical pulses have well-known benefits of compactness and environmental reliability compared to their bulk counterparts, as particularly advantageous for practical applications. The demonstrated combination of fiber laser and OP-GaAs technologies promises a truly practical source of THz radiation.

The experimental setup for THz generation and characterization is shown in Fig. 10. The optical pump source was an all-fiber laser that produced 120-fs pulses at 100 MHz repetition rate with the average power of 3 W (30 nJ pulse energy) at the wavelength of 1980 nm. Briefly, output of a mode-locked Er-fiber oscillator at 1557 nm was amplified in an Er/Yb-doped fiber amplifier, then Raman-shifted to 1980 nm, and finally amplified a large-mode-area Tm-doped fiber amplifier. The details of the system architecture and the performance achieved are reported in ref. 6.
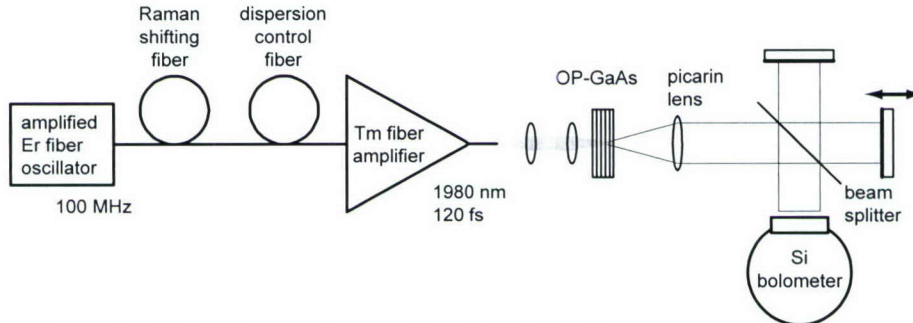

Fig. 10. Schematic of the THz experiment with a fs-Tm-fiber laser.

We used two OP-GaAs samples (D3 and E3) grown by epitaxy. Both samples were 0.4-mm-thick and 3-mm-long, and had lithographically-defined QPM periods of 1277 mm (sample D3) and 759 mm (sample E3). The pump beam was propagating along the [110] direction of GaAs and was polarized along [111] to maximize the effective nonlinear optical coefficient.

The focusing of the pump beam was optimized to produce the maximum THz power. The resulting optimal spot size was found to be $w_0 = 65$ μm which in agreement with theoretical predictions.[3] The generated THz beam was collimated with a Picarin plastic lens that had a focal length of 50 mm. THz power was measured with a Si bolometer.

In order to measure spectral properties of the generated THz radiation we used a Michelson interferometer, described above. For the sample D3, the spectrum was centered at 1.78 THz and has a width of 0.3 THz, while for the sample E3 the spectrum was centered at 2.49 THz and has a width of 0.25 THz, in good agreement with predicted QPM peak position and width.

Fig. 11 shows the measured THz power versus the incident optical power at 1980 nm. Both samples show very similar power-curve behavior: at the highest optical power of 2.1 W available at the samples we obtained ~ 3.3 μW of THz average power. The THz output power is quadratic with respect to the incident pump power and does not show any saturation effects, up to the maximum pump power of 2.1 W at the samples (peak intensity inside the samples of 1.85 GW/cm^2).
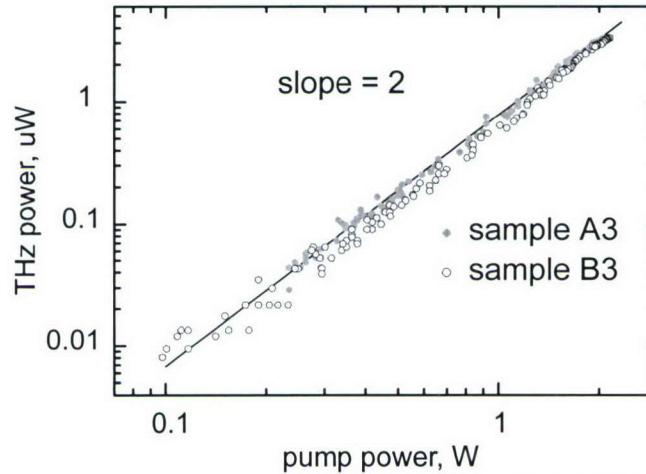

Figure.11. THz average power versus average pump power for the OP-GaAs samples D3 (filled circles) and E3 (open circles). Straight line is the best fit to the sample D3 data.

The maximum optical-to-THz efficiency achieved was 1.6×10^{-6}. Here we note that the OP-GaAs samples were not antireflection-coated and the Fresnel losses at optical and terahertz frequencies exceeded 30% per surface. Thus, the internal THz efficiency was calculated as 4.7×10^{-6}, corresponding to the internal normalized efficiency of 2.24×10^{-4} μJ^{-1}. The conversion efficiencies achieved in these experiments are about 25% of the ideal calculated values[3]. The discrepancy can be accounted for by several factors, namely, clipping of the generated THz beam because the wavelength of the THz wavelength is comparable to the sample thickness (0.4 mm); attenuation of THz radiation in air due to water vapor absorption; the pump pulses being about twice the transform limit and not having the ideal Gaussian shape as was used in the theoretical calculations.

Although we have used OP-GaAs samples with the fixed QPM periods, however the lithographic nature of fabrication readily allows to fabricate multiple QPM grating segments or even a fan-out QPM gratings, so that continuous THz frequency tuning can be achieved by transverse translation of the sample.

3. THz generation using picoosecond OPO

With the femtosecond excitation, the limit for THz efficiency is set by parasitic high-order nonlinear effects (e.g. nonlinear refraction). The optical-to-THz efficiency can be improved by using a two-color DFG scheme with longer (ps) pulses [3].

Our approach to generating quasi–monochromatic THz radiation was to use frequency mixing between the signal and idler waves of a synchronously pumped optical parametric oscillator (SPOPO). The SPOPO was run in two configurations: the singly resonant oscillator (SRO) resonantly enhanced only one wave (signal in our case) to very large intracavity powers, and the doubly resonant oscillator (DRO) enhanced both the signal and the idler. The pump source for the OPO was a Nd:YVO$_4$ CW–modelocked solid–state laser (picoTRAIN, High Q Laser) with a 50–MHz pulse repetition rate, 7–ps pulsewidth, 1064–nm wavelength, 10–W average output power, and horizontal polarization. The linear cavity length was 3 m with a roundtrip time equal to the period between pump laser pulses. For the OPO gain medium, we used an anti–reflection (AR) coated (for pump, signal, and idler) MgO–doped PPLN crystal, with a QPM period of 14.1 μm.
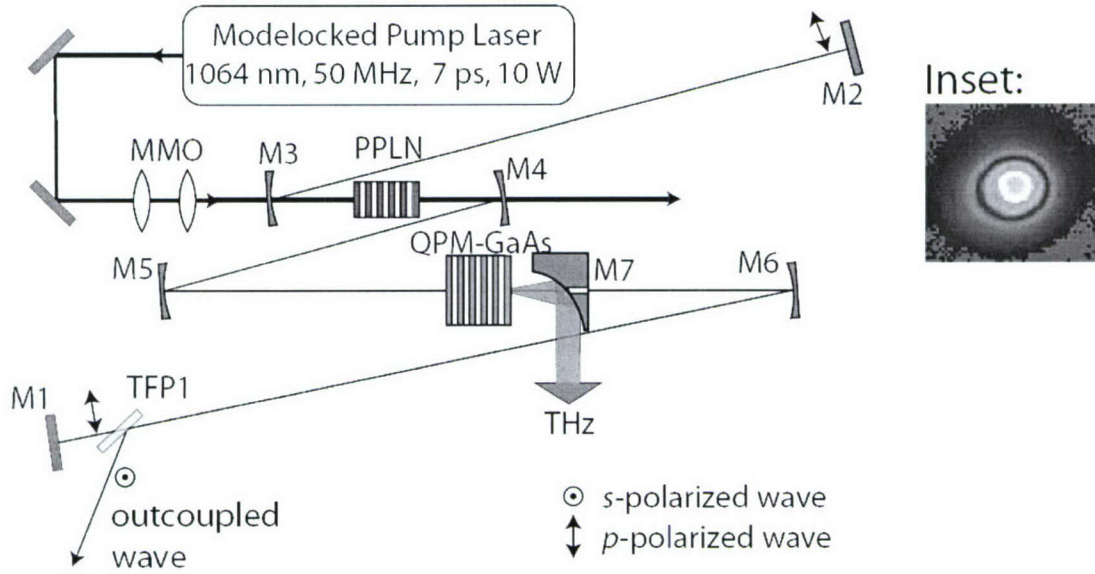

Fig. 12. Schematic of the linear SRO THz generation setup. Inset: Excellent TEM00 oscillating cavity mode intensity profile as measured at M6 with a 1:1 imaging lens and room–temperature pyroelectric camera.

The OPO was designed for type–II (o–oe) QPM parametric interactions, to allow narrow OPO signal and idler spectra near degeneracy, $\lambda s \approx \lambda i \approx 2\lambda p$ (here $\lambda p < \lambda s < \lambda i$ are the pump, signal, and idler wavelengths respectively).The nonlinear–optical coefficient for type–II phasematching was 5× less ($d_{31} = 2.37$ pm/V)

than the typical type–0 (e–ee) coefficient (d_{33}), which resulted in a parametric gain reduced by a factor of 25 compared to the usual type–0 configuration.

A thin–film plate polarizer, TFP1, separated the signal and idler waves directing the p–polarized wave to cavity end mirror M1 while the s–polarized wave was out-coupled from the OPO (p–polarization with respect to TFP1 corresponds to o–wave with respect to the PPLN crystal). The front surface of TFP1 was AR–coated for p–polarized transmission and s–polarized reflection, and the angle of incidence was 55° which was the brewster's angle for transmission of the p–polarized optical wave through the back surface. The mode–matching optics (MMO) consisted of a beam expander and focusing lens (3–lens system) for precise mode matching of the pump, signal, and idler inside the PPLN crystal. The focused pump spot size (1/e2 intensity radius) at the center of the PPLN was w = 30 μm. Mirrors M1 and M2 were end mirrors for the o–wave (Fig. 12). Mirrors M3 and M4 were separated by 21.3 cm and had 20–cm radii of curvature (ROC) which created a signal and idler spot size of 57 μm in the center of the PPLN. A second position for focused signal and idler beams (140 μm) was created using mirrors M5 and M6, which were separated by 50 cm and had 50–cm ROC. The distance between mirrors M4 and M5 was 30 cm, and the remaining cavity single–pass length of ~200 cm was divided evenly into the two end lengths (M6–M1 = M3–M2). The THz wave was extracted from the SRO by mirror M7, which was a gold–coated 90°–off–axis parabolic mirror with a focal length of 5 cm placed ~5 cm after the QPM GaAs crystal, which created a well–collimated, nearly diffraction limited THz beam. The THz wavelength was roughly 100× larger than the optical wavelengths, therefore it had a diffraction cone which was also 100× larger. A 3–mm–diameter hole was drilled through M7 to fully transmit the optical waves oscillating inside the cavity. M7 out-coupled > 90% of the THz wave from the cavity. All mirrors, except M7, were AR–coated for the pump and HR–coated for the signal and idler waves with a reflection loss < 0.1%.

For this section, we consider the SRO performance without GaAs and M7 inside the cavity. In the SRO configuration, the e–wave was out-coupled from the OPO cavity every roundtrip, while the o–wave was resonantly enhanced inside the cavity. The oscillating wave had a nearly radially symmetric intensity profile (TEM$_{00}$ mode) indicating good cavity alignment and mode matching of the pump and signal inside the PPLN (Fig. 12 inset).

Fig. 13a shows measured wavelengths for the o– and e–waves set by the temperature of the PPLN crystal. The e–wave was measured from the power outcoupled from the cavity by TFP1, and the o–wave was measured by the small amount of power transmitted through M1. The data are fitted by (solid lines) second–order polynomial expressions. There is no reliable reference for temperature–dependent index of refraction for for both of the o– and e–waves in 5% MgO:PPLN. The OPO tuning characteristics were measured as a function of the PPLN temperature with a grating monochromator. Fig. 13b shows OPO lineshapes near degeneracy for two different PPLN temperatures. The FWHM linewidth was typically 1.5–3 nm for various PPLN temperatures with an average of 2 nm (130 GHz). For the SRO case, the outcoupled e–wave average power, resonated o–wave average power, and pump depletion can be measured and then used to calculate the roundtrip intensity loss (α) of the OPO for the resonated signal wave.
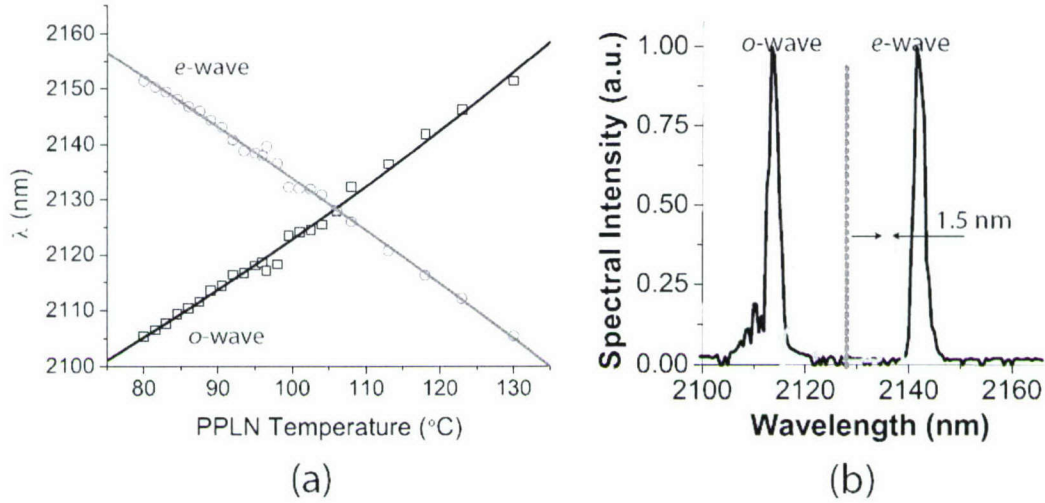
Fig. 13. (a) Type–II PPLN temperature tuning curves for both o–wave and e–wave (measured data points and solid–line polynomial fits). (b) PPLN OPO lineshapes near degeneracy for two different PPLN temperatures: t = 90 °C (frequency splitting of 2.05 THz, black lines) and t = 100 °C (frequency splitting of 0.96 THz, gray lines). The dotted line represents the degeneracy point (2128 nm).
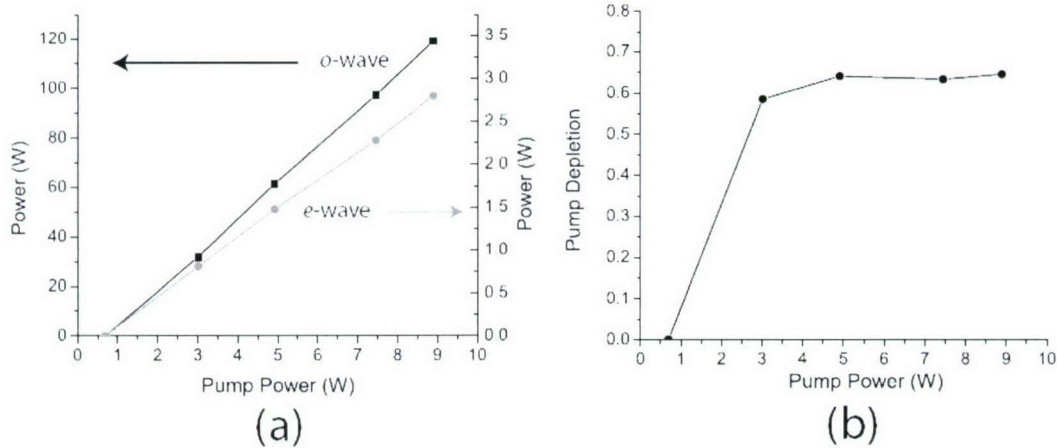

Fig. 14. (a) SRO average powers in the o–wave and e–wave versus average pump power at PPLN temperature of 83 °C reached 119 W and 2.79 W average powers, respectively. (b) At this same PPLN temperature the maximum pump depletion was 64.5%.

Pump depletion of the OPO is a measure of how many pump photons are parametrically converted to signal and idler photons per pass. The best SRO performance at a PPLN temperature of 83 °C achieved 119 W of average power in the o–wave, 2.79 W in the e–wave and depleted 64.5% of the pump wave. The OPO achieved threshold with 0.69 W of average pump power (Fig. 14). At a MgO:PPLN temperature of 83 °C the signal and idler wavelengths were 2107 nm and 2150 nm, respectively. Using Eq. 3, the calculated SRO loss without GaAs inside the cavity was 2.4%. This was a reasonable loss calculation considering a ~0.1% loss at each reflection and interface in a cavity with 10 mirror reflections

and 8 interfaces (interfaces of PPLN and polarizer) in one roundtrip. Assuming 9 W of average pump power is incident on the PPLN, 2.4% roundtrip intensity loss for the resonated wave, and 64.5% pump depletion, as an energy conservation check Eq. 4 yields an average resonated power of 122 W which is within 3% of the measured average power of 119 W. Thus, the SRO operated within a few percent of theoretical predictions.

THz generation outside the OPO cavity

We first generated THz radiation outside the cavity of the SRO. Without the resonant enhancement of the optical cavity the THz power levels were low, as expected; however, we were able to measure the QPM tuning curves of many samples and compare them to the theoretical predictions for phasematching center wavelengths. Fig. 15 shows the schematic for the extracavity experiments. The SRO signal and idler waves were out-coupled from the cavity using TFP1 at an angle of incidence of 51.5°, which was away from the ideal SRO operating angle of 55°. This created a loss for the o–wave in the SRO, but this out-coupled o–wave power was necessary so that both signal and idler were focused into the GaAs sample. Since the THz power scaled with the product of the two input beam powers, it was advantageous to create a higher loss SRO and gain higher product of extracavity signal and idler powers. A long–pass filter (LPF) which transmitted 50% at 1890 nm followed TFP1 with a transmission of 89% for $\lambda > 1.9$ μm. L1 focused the signal and idler beams in the QPM GaAs. The focused spot sizes for the two 2–μm beams were 80 μm.
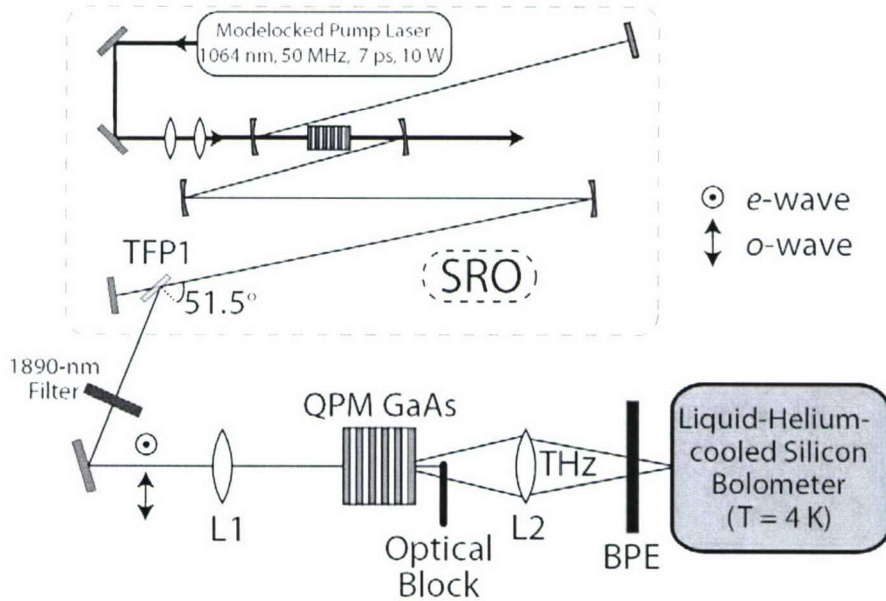

Fig. 15. Schematic of experiments which generated THz radiation outside the cavity of the SRO. The signal and idler (o–wave and e–wave, respectively) were outcoupled from the SRO and focused into various QPM GaAs samples. L1 was a signal and idler focusing lens, and L2 was a Picarin lens which focused the THz beam onto the liquid–helium–cooled silicon bolometer.

THz radiation was generated via DFG inside the QPM GaAs sample. The optical beam diffraction cone was ~100× smaller than the THz beam diffraction cone, and the optical beam was blocked by a small metal wire located directly after the GaAs crystal. The majority of the THz wave passed over the metal wire and was focused by a Picarin lens (L2, THz transmission ~40%) onto a liquid–helium–cooled silicon

bolometer (T = 4 K). A black polyethylene filter (BPE) (500 μm thick) was placed directly before the bolometer and blocked the remaining IR and visible radiation.

At a PPLN temperature of 86 °C, the combined signal and idler average power after the LPF was 750 mW, with 5× more signal than idler. Fig. 16a shows the measured THz QPM tuning curves of GaAs samples I3, I5, and I10 having the same QPM period of 704 μm but and different crystal lengths of 3, 5, and 10 mm. Since the QPM acceptance bandwidth scales inversely with the length of the QPM crystal, L, we see that the sample I3 has much (about 3 times) larger bandwidth than the sample I10. In Fig. 16b, the THz QPM tuning curves are shown for QPM GaAs samples H10, I5, and F5. The THz center frequency decreased with increasing the QPM period, in accord with theory.

The THz average power generated by sample I5 (~2.4 THz) at the PPLN crystal temperature of 86 °C was measured as the SRO signal and idler average powers were attenuated with a variable reflector wheel placed directly before the LPF. Since the THz average power scales with the product of the signal and idler average powers, it was expected that the THz average power scale quadratically with the 2–μm average power. The logarithmic plot in Fig. 17, with a slope of 2.05, shows that the THz average power did correctly depend quadratically on the 2–μm average power.
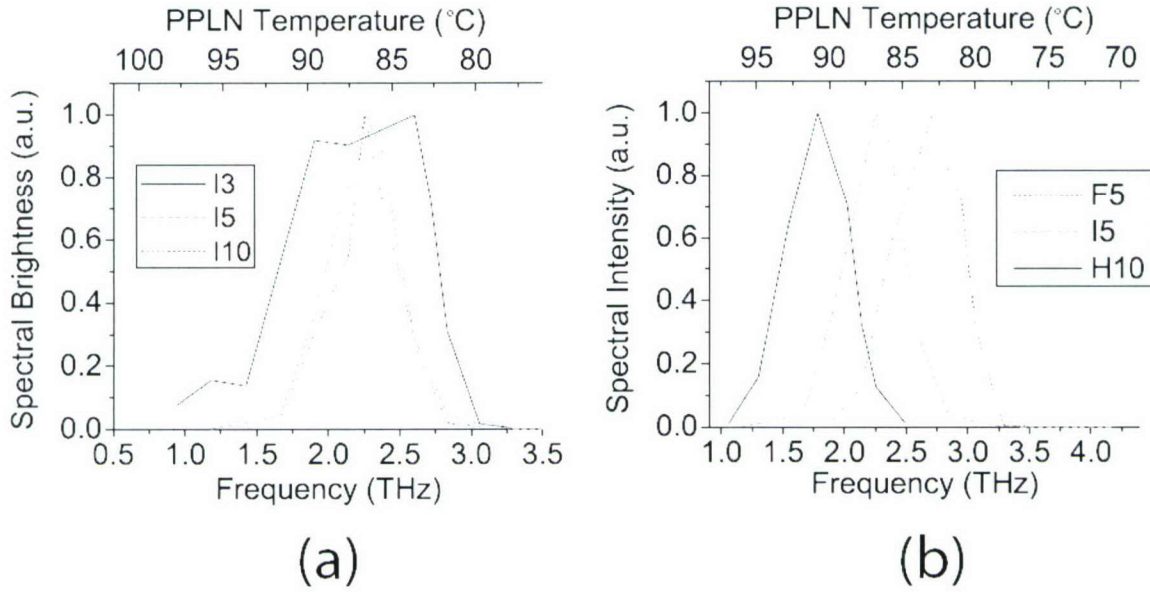

Fig. 16. (a) Measured THz QPM tuning curves for OP–GaAs samples with a QPM period of 704 μm and crystal lengths of 3, 5, and 10 mm (samples I3, I5, and I10, respectively). (b) Measured THz QPM tuning curves for OP–GaAs samples H10, I5, and F5.
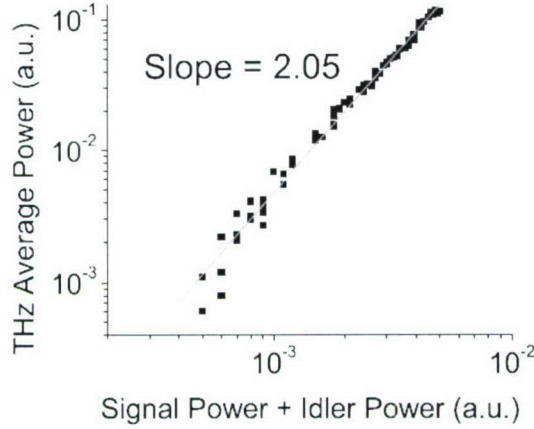
Fig. 17. The THz average power scaled quadratically with the signal and idler average powers as expected from THz difference–frequency mixing theory. The slope on the logarithmic horizontal and vertical axes was close to 2.

THz generation inside the cavity of a singly-resonant OPO

By placing the GaAs sample inside the cavity the optical–to–THz conversion efficiency increases since it scales with the product of the signal and idler powers. With the OPO operating in the SRO configuration where the e–wave was outcoupled every roundtrip by TFP1, the o–wave was resonantly enhanced with an enhancement factor of ~ $1/\alpha$. The cavity HR mirrors had reflection losses < 0.1%, and the AR–coated PPLN crystal had reflection losses < 0.5% per interface in the 2–μm band. The measured roundtrip intensity loss for the o–wave of 2.4% (see above) corresponded well to these losses given for one roundtrip there were 10 mirror reflections, 4 PPLN crystal interface transmissions, and 4 polarizer interfaces.

We positioned GaAs halfway between M3 and M4 the signal and idler had spot sizes of ~140 μm. Assuming that the signal and idler pulsewidths were similar in length to the pump pulsewidth (7 ps), the generation of THz via intracavity DFG follows theory taking into account temporal pulse walkoff, gaussian beam focusing, and quasi-phasematching. Fig. 18 shows the SRO as well as the equipment used to manipulate and measure the THz beam average power. The THz wave was generated inside the QPM GaAs crystal which was inside the SRO. The THz wave diffracted into a large cone and filled the aperture of M7 and was reflected towards L2. The THz beam was well–collimated before L2, and it was focused onto a room–temperature DLaTGS pyro–electric detector (Bruker Optics). The visible and IR radiation was blocked by a set of 2 black polyethylene (BPE) filters which transmitted > 50% for vTHz < 3 THz. With QPM GaAs sample A (DB–GaAs) placed inside the SRO the measured THz average power was 50 μW at 2.8 THz. For a pump power of 10 W, this is an optical–to–THz conversion efficiency of 5×10^{-6} and quantum efficiency of 5×10^{-4}. Fig. 19a shows the THz–beam intensity profile after collimating mirror M9, reconstructed from scanning knife–edge measurements. Horizontal and vertical 1/e2 spot sizes of 7.8 mm and 13.3 mm, respectively, were close to the diffraction limit. The focused THz beam was captured (Fig. 19b) by a room–temperature pyroelectric camera (Pyrocam III, Spiricon). The focused

beam spot is 2–3 pixels (1 pixel = 100 μm ×100 μm), which again confirms nearly diffraction–limited performance.
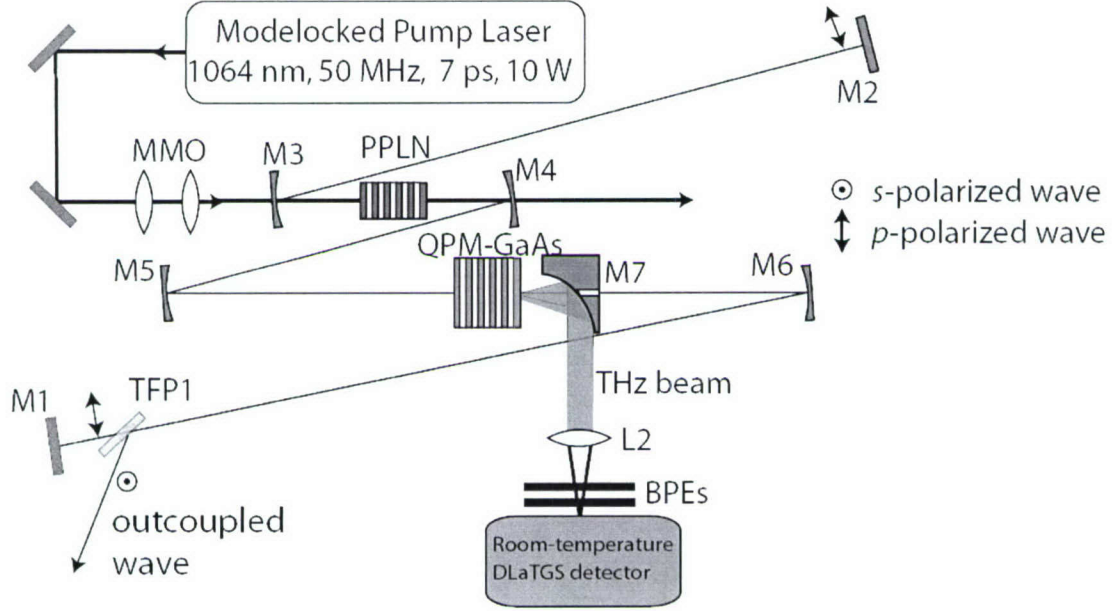

Fig. 18. Schematic of measurements of THz average powers generated via intracavity DFG in the SRO configuration. The THz beam was outcoupled by M7, focused by Picarin lens L2, and measured with a room–temperature DLaTGS pyro–electric detector.
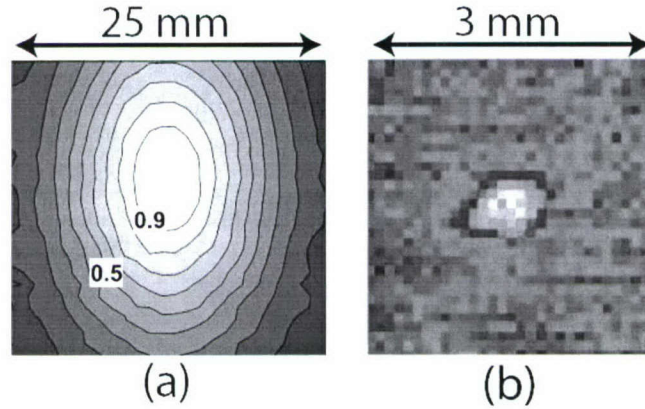

Fig. 19. (a) The collimated THz–beam intensity profile reconstructed from scanning knife- edge measurements. (b) The focused (Picarin f = 5 cm lens, L2) THz–beam intensity profile measured by a room-temperature pyroelectric camera (1 pixel = 100 μm ×100 μm).

Intracavity temperature tuning curves were measured for many QPM GaAs samples and with higher signal–to–noise ratios since the THz average powers were larger than was the case for the extracavity experiments. Fig. 20a shows the measured THz QPM tuning curves for samples A, C, L5, and M5. The horizontal axis is the THz frequency as calculated from the OPO signal and idler tuning curves of Fig. 13a. The PPLN crystal temperature is translated to a difference frequency (THz frequency) between the SRO o– and e–waves. The center PPLN crystal temperatures (center THz frequencies) of the tuning curves agreed well with the calculated values. The clipping losses induced by passing the 2–μm beams with cavity spot sizes of ~150 μm through samples with apertures < 600 μm (in either transverse dimension) were too great; therefore, only DB–GaAs, OC–GaAs, and the thickest OP–GaAs samples were useful for SRO intracavity THz generation. Table 2 shows the SRO signal average power, idler average power, threshold, and maximum pump depletion values for the THz–generating samples placed in the SRO. The best THz performance in the SRO configuration occurred with sample A (QPM period of 504 μm) which generated quasi-monochromatic THz radiation with a center frequency of 2.8 THz and FWHM spectra bandwidth of ~300 GHz (calculated). The center frequency matched well with the theoretical QPM calculations. Sample A generated 50 μW of average output power (after M7) in a nearly–diffraction limited beam. The SRO signal and idler powers were 11.1 W and 2.2 W, respectively, at a maximum pump average power of 8.9 W.

Table 2. SRO Intracavity THz Generation Performance

Sample	Signal Power (W)	Idler Power (W)	Threshold (W)	Pump Depletion (%)
1 mm thick GaAs wafer	60.9	2.51	1.03	59
A	11.08	1.74	3.74	43
C	43.2	2.1	0.94	55.7
M5	11.2	1.7	2.05	51
L5	15.3	2.16	2	59
L10	7.8	1.43	2.04	43
K10	4.6	1	2.9	33

Interestingly, we also observed (like in the case with fs pulses described above) the higher–order QPM tuning curves for samples B and C. Fig. 21 shows the 1st, 3rd, and 5th–order (m = 1, 3, and 5) QPM tuning curves for sample C with center frequencies of 0.62 THz, 2.24 THz, and 3.32 THz, respectively. The center frequencies do not scale exactly with m because there is a finite GaAs dispersion between 0.5–4 THz. This OPO–based THz source allowed for a single QPM GaAs sample to generate three different THz frequencies simply by changing the temperature of the PPLN crystal.
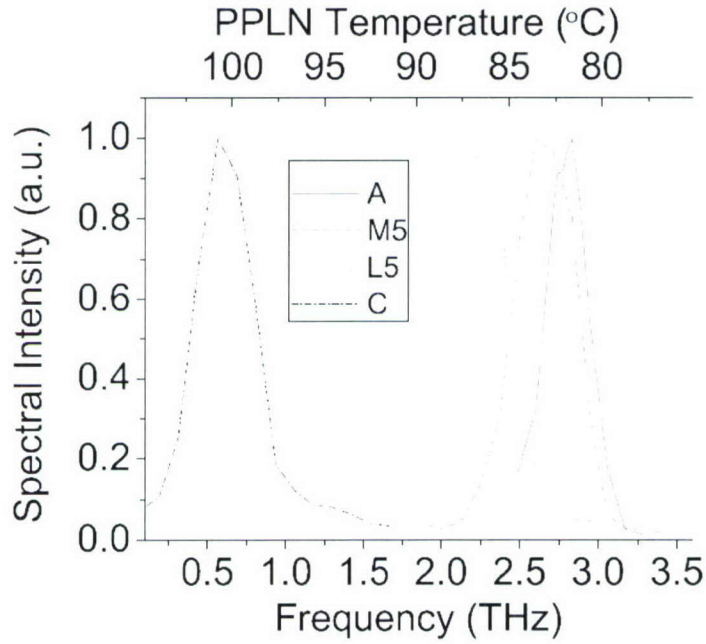
Fig. 20. Measured THz QPM tuning curves for QPM GaAs samples A, C, L5, and M5 showing tunability of THz output frequency by using GaAs samples with different QPM periods.
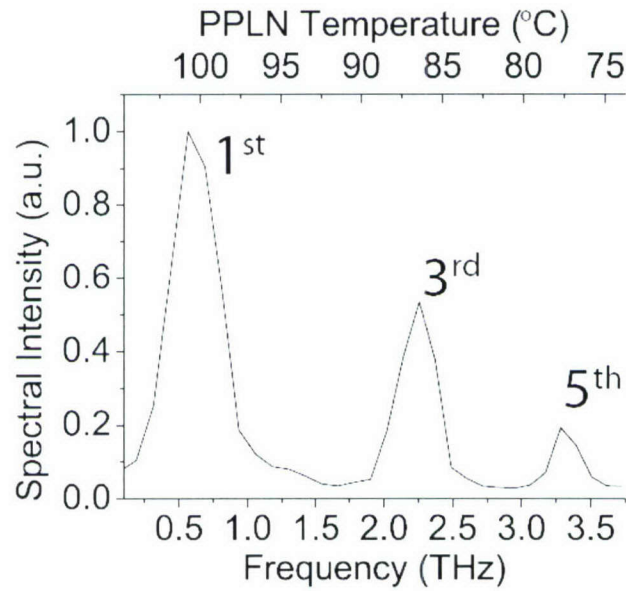

Fig. 21. 1st, 3rd, and 5th–order QPM with sample C allowing generation of three different THz frequencies (0.62 THz, 2.24 THz, and 3.32 THz, respectively) with a single QPM GaAs sample.

Observation of THz cascading effect during optical-to-THz frequency conversion

Our parametric frequency down–conversion source of THz radiation transferred energy from waves in the 2–µm band to a THz wave. In quantum–mechanical terms, two lower–energy photons were generated from a destroyed largest–energy photon. This down–conversion took place in the QPM GaAs crystal, and the three waves were the OPO signal, OPO idler, and THz waves.

The THz wavelength is in our case ~100× larger than the signal and idler wavelengths, which meant that the THz photon energy was ~1% of the signal and idler photon energies. If the difference–frequency mixing depleted all of the optical pump (all of the energy in the signal wave was transferred to the idler and THz waves) then the optical–to–THz conversion efficiency was only 1%. In order to improve this efficiency we proposed a cascaded difference–frequency mixing process where the overall conversion efficiency scales with the number of cascades. Fig. 22 illustrates how energy flows from the higher energy waves to the lower energy waves. Each cascading process adds energy to the THz wave at a set THz frequency increasing the overall conversion efficiency. Cascading can occur between phasematched waves, and theoretically the number of cascades, N, can be on the order of the ratio of GaAs acceptance bandwidth to the THz frequency. Previously, we noted that the THz wave was the same polarization as the OPO e–wave, in agreement with theory and due the symmetry of the GaAs $\chi(2)$ tensor. This also meant that the 2–µm waves (signal, idler, and subsequent satellites) must alternate polarizations. By rotating TFP by 90°, the SRO resonantly enhanced the idler (e–wave), and the PPLN crystal temperature was set to 82.3 °C for generation of 2.8 THz using sample A.
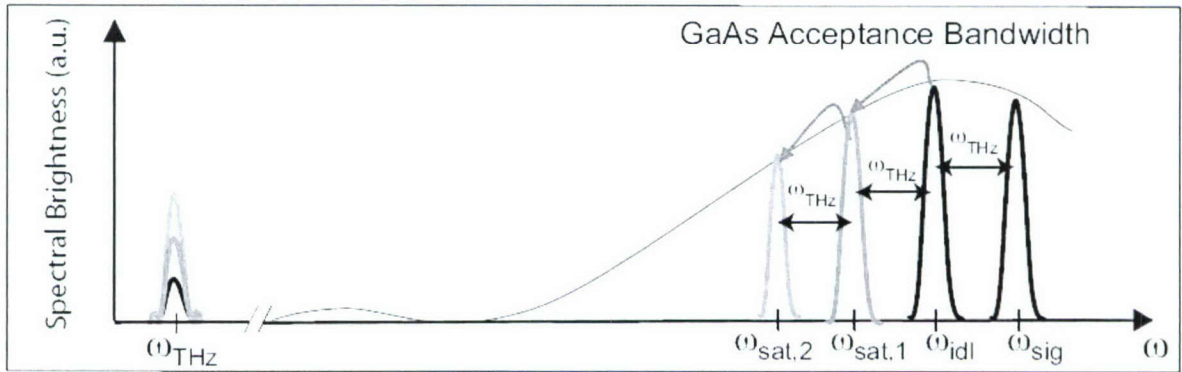

Fig. 22. Parametric down–conversion and cascading showing amplification of the THz spectra after each cascading process (generation of each satellite). The two farthest right line-shapes are the SRO signal and idler, respectively, and the farthest left line-shape is the THz spectra.
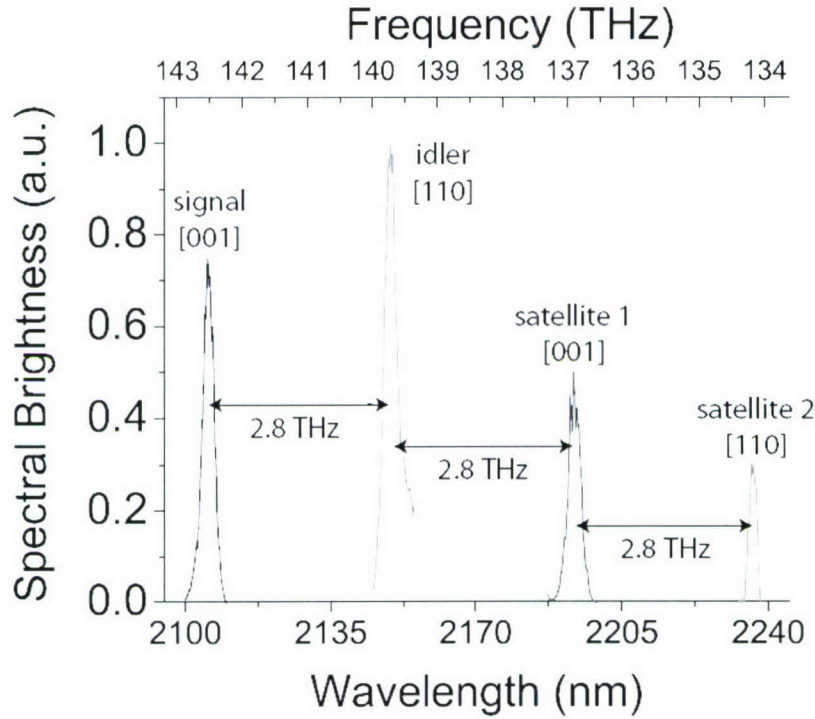
Fig. 23. Measured cascading in the SRO configuration with the idler wave resonantly enhanced. The waves were spaced by 2.8 THz, as expected, and the field polarizations alter- nated between GaAs crystalline directions [110] and [001].

Using a diffraction grating monochromator we measured the OPO spectrum consisting of signal, idler, and plus two red-shifted cascades (Fig. 23) around 2100–2200 nm. The generated THz wave was measured separately by the DLaTGS detector. The vertical scaling was adjusted to convey the relative strengths of the 4 waves, with the strongest wave being the resonantly enhanced idler. All optical waves were outcoupled by SRO mirror M1. In agreement with theory, the spacing between any two waves was 2.8 THz, and adjacent (in frequency) fields had orthogonal polarizations (along either [110] or [001] GaAs crystalline directions). These results proved that cascading occurred as predicted, however, the optical–to–THz conversion efficiency was not significantly improved since each subsequently generated satellite decreased in energy. Having satellite waves with energies comparable to the signal and idler will require all 2–µm waves to be resonantly enhanced by the optical cavity. A design to improve conversion efficiency using resonantly enhanced is currently being implemented in Phase 1B.

THz generation inside the cavity of a doubly-resonant OPO

In the SRO configuration, using sample A, we generated 50 µW of average output power at 2.8 THz with 5× more signal power than idler power. From theory, the THz average power scales linearly with the product of the signal and idler powers and therefore will be maximized when the signal and idler powers are maximized and equal. By resonantly enhancing both the signal and idler waves using the optical cavity, the optical–to–THz conversion efficiency was increased by 20× over the previous SRO results. We also reduced as much as possible the losses of the cavity for both the signal and idler waves since the efficiency scaled inversely with the square of the roundtrip intensity losses in the DRO.

Fig. 24 shows the DRO configuration with the addition of two mirrors (M3 and M4) and a second polarizer (TFP2). The spot size of the focused 1–µm pump beam in the center of the PPLN crystal was 30 µm, while the calculated focused waists of the resonating DRO modes in the PPLN center were 57 µm. Two thin–film polarizers, TFP1 and TFP2, separated the orthogonally polarized signal and idler waves. Mirrors M5 and M6 were concave with 200–mm radii of curvature (ROC), and mirrors M7 and M8 were concave with 500–mm ROC. QPM GaAs sample A, AR coated for the 2–µm band, was placed near the focused signal and idler waists (140 µm, calculated) between mirrors M7 and M8. To avoid back–conversion of the signal and idler on the return pass in the PPLN, we made distances TFP1 − M1 and TFP1 − M3 unequal. In order to keep the roundtrip times for the signal and idler waves equal, the paths TFP2−M2 and TFP2−M4 were correspondingly adjusted. In this "offset" cavity design, the signal and idler waves perfectly overlap in time during their forward pass through the PPLN; however, they do not overlap during the return pass, where otherwise the signal and the idler would back- convert to 1-µm photons by sum-frequency generation. By applying dithering to one end mirror at ~100 Hz with a piezoelectric actuator, we achieved DRO oscillation with a duty factor > 30%. Since the DRO resonated simultaneously at two different frequencies (signal and idler), the difference of the lengths of both cavities, at the point of double resonance, required stabilization to ~100 nm. A cavity–length stabilization scheme with a servo loop to achieve true continuous–wave operation is under development (Phase 1B). The best THz performance in the DB-GaAs occurred when the OPO was tuned to $\lambda s = 2107$ nm and $\lambda i = 2150$ nm ($t = 82.7$ °C), corresponding to a difference frequency of 2.8 THz. This agreed with the calculated, as well as measured [2] GaAs QPM peak position at a QPM period of 504 µm. Our estimate of the THz–wave bandwidth of 300 GHz was based on optical–wave linewidth measurements. The polarization of the THz beam was again measured to be along the [110] crystalline direction of GaAs, in agreement with the symmetry of the EO tensor. The THz average power was measured with a calibrated DLaTGS pyroelectric detector (Bruker Optics) and black polyethylene filters, which blocked the optical radiation. The largest THz average output power of 1 mW was achieved when the DB-GaAs was placed 2 cm beyond the focused signal and idler beam waists (towards M8) at a position where the spot sizes were each 173 µm. The THz output generated via DFG scales as the product of the OPO signal and idler powers. In the DRO case, it is expected to scale as the inverse square of the cavity loss. The OPO mirrors plus the PPLN crystal introduced roundtrip intensity losses of only 2.5%. The largest contributions to roundtrip loss came from QPM GaAs sample A (12%) and the two polarizers (6–8%); therefore, the total roundtrip intensity loss exceeded 20% for each resonating wave. At an average pump power of 8.5 W (the DRO threshold was 2.4 W), the pump depletion was 67%, and the intracavity signal and idler average powers were measured to be 10.2 W and 17 W, respectively. Assuming that the signal and idler had the same pulsewidth as the pump, we found that the generated 1 mW of THz output power was within ±10% of theoretical predictionsbased on ref. 3, with an optical–to–THz efficiency of 1.2×10^{-4} (quantum efficiency of 1.2%).
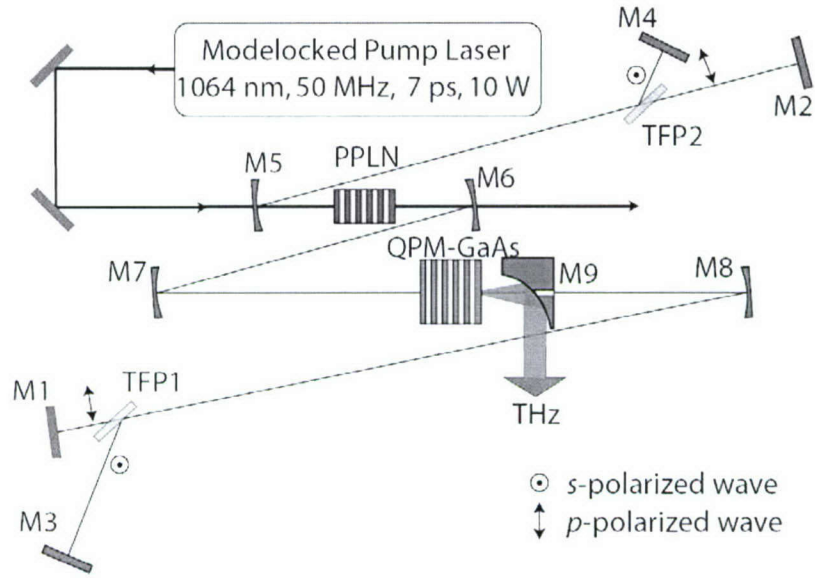
Fig. 24. Schematic of the linear DRO with an "offset" cavity design. M1–M8 were cavity mirrors, and M9 was an off-axis parabolic mirror for THz outcoupling.
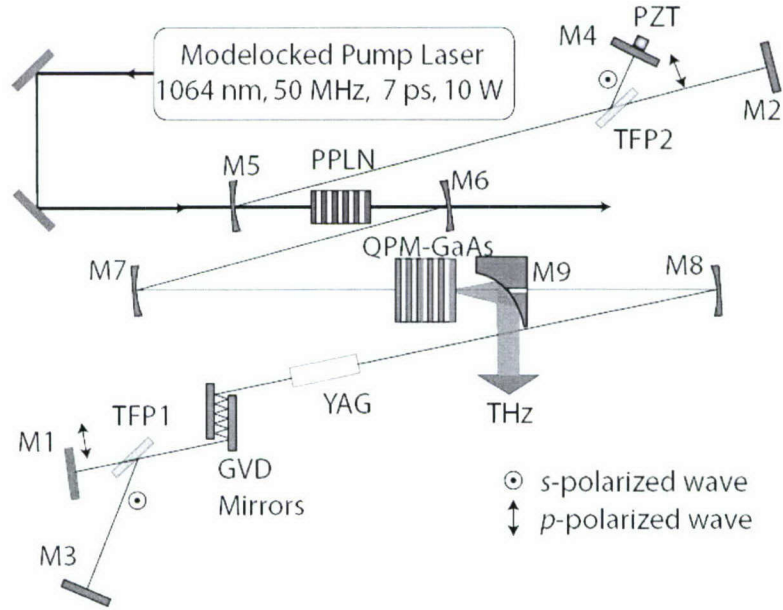

Fig. 25. GVD–compensated DRO using bulk a bulk YAG crystal and multiple–bounce GVD–coated mirrors to achieve the correct amount of compensation. This cavity is length–stabiized using a feedback loop with actuator, PZT, to length–stabilize the cavity lengths to sub–λ accuracy.

4. Future Work and Conclusion

In order to reach THz average powers of 100 mW, we must first stabilize the DRO by implementing a dither– and–lock stabilization system which operates the DRO in CW–mode. We will then increase the generated THz power by designing resonantly enhanced cascading. In order for all optical waves (signal, idler, and cascades) to be enhanced by the optical cavity, they must resonate simultaneously. To achieve this goal, one needs to compensate group–velocity dispersion (GVD) in such dispersive media as PPLN and GaAs. This can be done by using special "GVD-compensating" mirrors and by inserting into the OPO cavity additional bulk optical elements with the opposite sign of GVD, as compared to that of GaAs + PPLN - in order to "re–align" the phase of the optical pulses in each roundtrip. Thus, a final setup may be as shown in Fig. 25. Current designs will resonate the signal, idler, and 8 cascades and generate > 50 mW of average output power at 1.5 THz using OC–GaAs (QPM period 1-1.5 mm) as the frequency mixer.

References

[1] T.J. Bridges, A.R. Strnad, Submillimeter wave generation by difference-frequency mixing in GaAs, Appl. Phys. Lett. 20, 382 (1972).

[2] K. L. Vodopyanov, M. M. Fejer, Y.-S. Lee, W. C. Hurlbut, V.G. Kozlov , Terahertz wave generation in quasi-phase-matched GaAs, *Appl. Phys. Lett*, 89, 141119 (2006)

[3] K. L. Vodopyanov, "Optical generation of narrow-band terahertz packets in periodically inverted electro-optic crystals: conversion efficiency and optimal laser pulse format," Opt. Express 14, 2263-2276 (2006

[4] T. Skauli, P. S. Kuo, K. L. Vodopyanov, T. J. Pinguet, O. Levi, L. A. Eyres, J. S. Harris, M. M. Fejer, *J. of Appl. Phys.* 94, 6447-55 (2003).

[5] G. Imeshev, M. E. Fermann, K. L. Vodopyanov, M. M. Fejer, X. Yu, J. S. Harris, D. Bliss, C. Lynch, High-power source of THz radiation based on orientation-patterned GaAs pumped by a fiber laser, *Opt. Express* 14, 4439-4444 (2006)

[6] G. Imeshev and M. E. Fermann, 230-kW peak power femtosecond pulses from a high power tunable source based on amplification in Tm-doped fiber, *Opt. Express* 13, 7424-7431 (2005)